

# **E214 The ATLAS Experiment**

Alperen Esen  
s39aesen@uni-bonn.de

Benjamin Brandt  
s08bbran@uni-bonn.de

Date of experiment: 08-09.05.2025

Handed in: 30.05.2025

University Bonn – Physics Faculty

## Contents

<b>1. W-mass</b>	<b>3</b>
1.1. Electron Calibration Verification . . . . .	3
1.2. QCD scale factor and Kinematic Variables . . . . .	4
1.2.1. Kinematic Variables . . . . .	4
1.2.2. Final QCD scale factor . . . . .	8
1.3. Cut selection . . . . .	9
1.4. Gauge curves . . . . .	10
1.5. W-mass . . . . .	10
<b>A. Appendix</b>	<b>10</b>
<b>References</b>	<b>12</b>

# 1. W-mass

With the finished calibration, the mass of the W-boson can now be measured. This is done using the Jacobi peak of the electron transverse momentum distribution. In order to determine the W-mass, we use a data set of actual ATLAS data containing  $W \rightarrow e\nu$  events, as well as several simulated data sets also containing  $W \rightarrow e\nu$  events. There is also a  $Z^0 \rightarrow e^+e^-$  data set to check the validity of the previous calibration. Finally there are data sets for QCD- and non-QCD background events.

## 1.1. Electron Calibration Verification

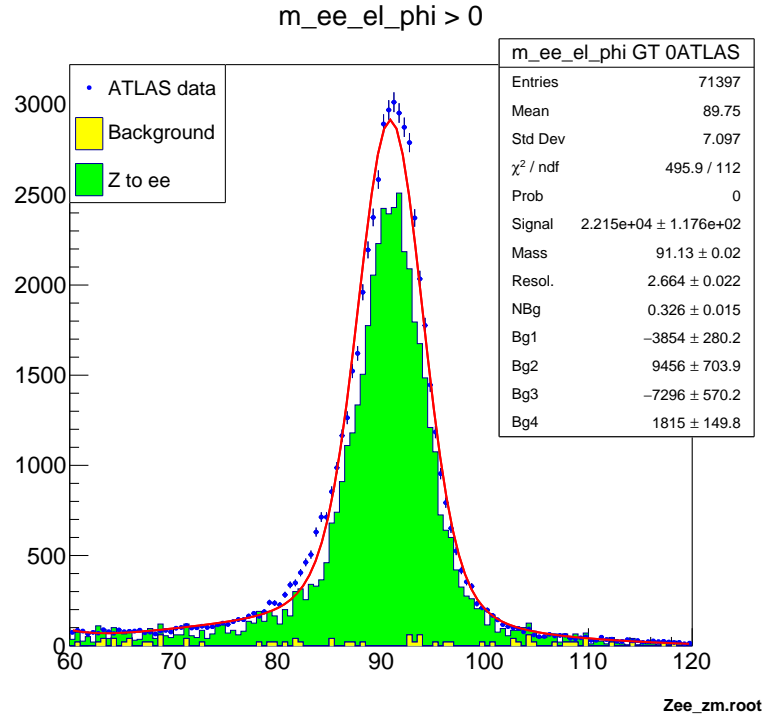


Figure 1:  $Z_{mass\_check\_e l_p t - cut.pdf}$

cut selection	$M_{Z^0, meas} / \text{GeV}$	$\left  \frac{M_{Z^0, meas} - M_{Z^0, lit}}{M_{Z^0, meas}} \right $
$p_{T, e^\pm} > 40 \text{ GeV}$	$91.71 \pm 0.02$	
$p_{T, e^\pm} < 40 \text{ GeV}$	$90.5 \pm 0.0$	
$35 < p_{T, e^\pm} < 55 \text{ GeV}$	$91.43 \pm 0.02$	
$\eta > 2$	$89.89 \pm 0.05$	
$\eta < 0.5 \ \& \ p_{T, e^\pm} > 40$	$91.69 \pm 0.02$	
$\eta < 0.5 \ \& \ p_{T, e^\pm} < 40$	$90.56 \pm 0.03$	
$\phi < 0$	$91.14 \pm 0.02$	
$\phi > 0$	$91.13 \pm 0.02$	

**Table 1:** Measured  $Z^0$  mass for different cut selections

## 1.2. QCD scale factor and Kinematic Variables

In order to achieve an accurate measurement of the W-mass, the background processes at ATLAS have to be taken into consideration. At LHC, proton proton collisions cause the measured events, therefore the background coming from QCD processes is large. This causes a problem, since the final products of the  $W \rightarrow e\nu$  events we use to measure the W-mass are leptons which do not interact with the strong interaction. This makes the simulation of a QCD background for the  $W \rightarrow e\nu$  events difficult. In order to solve this problem, the QCD background is extracted from the data. In order to scale the data correctly, a QCD scale factor is used, since the integrated luminosity of the background is not measured and therefore unknown. In order to get an understanding of the QCD scale factor and its effect on the data, different kinematic values are be plotted for different QCD scale factors.

### 1.2.1. Kinematic Variables

In order to get a feeling for the QCD scale factor and estimate its optimal value, different kinematic Variables are analyzed. The chosen kinematic variables are **e1\_pt** (the transverse momentum of the electron), **etmis** (missing transverse energy/momentum), **njet** (number of jets in the event) and **ptw** (transverse momentum of the W boson). The distributions of these different variables for a scale factor of 1 (meaning no scaling) can be seen in figure 6. From figure 6 it is obvious that the ATLAS data does not agree very well with the simulations. In order to solve this, the QCD scale factor was set to different values whilst looking at the distributions until the agreement between real and simulated data was optimal by eye. Compromises were necessary, since the alignment between real data and simulated data was unequal for different regions. After some trial and error, the optimal QCD scale factors the four mentioned kinematic variables were chosen as:

Variable	QCD scale factor
<code>etmis</code>	$0.30 \pm 0.05$
<code>el_pt</code>	$0.35 \pm 0.07$
<code>nejt</code>	$0.46 \pm 0.08$
<code>ptw</code>	$0.42 \pm 0.06$

**Table 2:** Optimal QCD scale factors for each of the examined kinematic variables.

The errors were chosen to account for the previously mentioned problem, that the data aligned unequally well with the simulated data in different regions of the distributions. Therefore the errors were chosen, such that at the end of the error interval, the alignment was best in one region whilst the disalignment in the rest of the distribution was still decent. Overall the kinematic variables display the expected behavior. The transverse momentum of the W-boson `ptw` is mostly small, meaning less than ca. 30 GeV. When looking at the electron transverse momentum `el_pt`, the  $W \rightarrow e\nu$  events display a peak between 40 and 50 GeV which is expected since this is around half the mass of the W-boson, which is coming from the Jacobi peak [1]. The increase towards lower  $p_T$  is mostly due to QCD background. When looking at the missing transverse momentum `etmis` the distribution behaves similarly to the electron transverse momentum `el_pt`, which is expected. Since the transverse momentum of the W-bosons is mostly small, compared to that of the from the decay resulting electron and neutrino, due to momentum conservation, the electron and the neutrino get approximately half the W-boson mass as energy. It is therefore expected that both these distributions, when disregarding the background, feature a peak located around the W-boson mass. The distribution

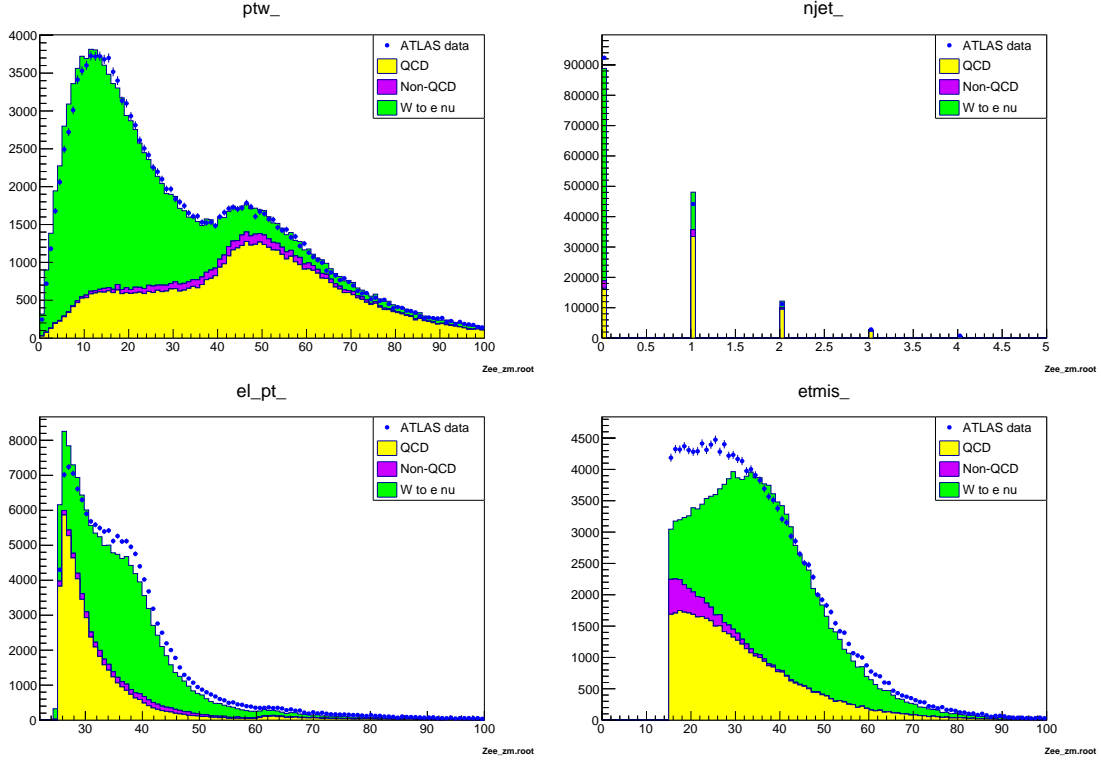


**Figure 2:** Distributions of the kinematic variables  $ptw$ ,  $njet$ ,  $el\_pt$  and  $etmis$  for the QCD factors mentioned in table 2

In the next step, the distribution of  $p_T^W$  is analyzed for events with different jet multiplicities. The corresponding histograms are displayed in figure 3. A clear trend is observed: the signal-to-background ratio decreases as the number of jets increases. This behavior aligns with the jet multiplicity distribution shown previously in figure 2.

For events with zero jets, the signal is dominant at low  $p_T^W$ , peaking around 10-15 GeV. This is expected, as there are no jets present to impart recoil to the W boson. However, when considering events with one jet, the signal drops significantly, and the previously observed peak at low  $p_T^W$  disappears. Instead, the signal appears relatively flat in the low to mid- $p_T^W$  range and then declines at higher values. This can be explained by the presence of one jet in these signal events, which imparts recoil to the W boson. Although the jet direction is unknown, assuming an isotropic distribution, this results in a roughly uniform  $p_T^W$  distribution. Lower  $p_T^W$  values correspond to a forward jet recoil, while mid to high  $p_T^W$  suggests more transverse recoil.

The background shows a noticeable increase around 50 GeV. This could be related to the W boson mass, as the peak occurs slightly above half its mass, although other factors may also contribute.

As the number of jets increases further, the signal continues to diminish while the background becomes more dominant. The background still peaks around 50 GeV, but the overall number of events decreases. This trend is consistent with expectations: the

original process does not favor the presence of jets, and the likelihood of additional (radiated) jets decreases with increasing event complexity, due to a reduction in available vertices.

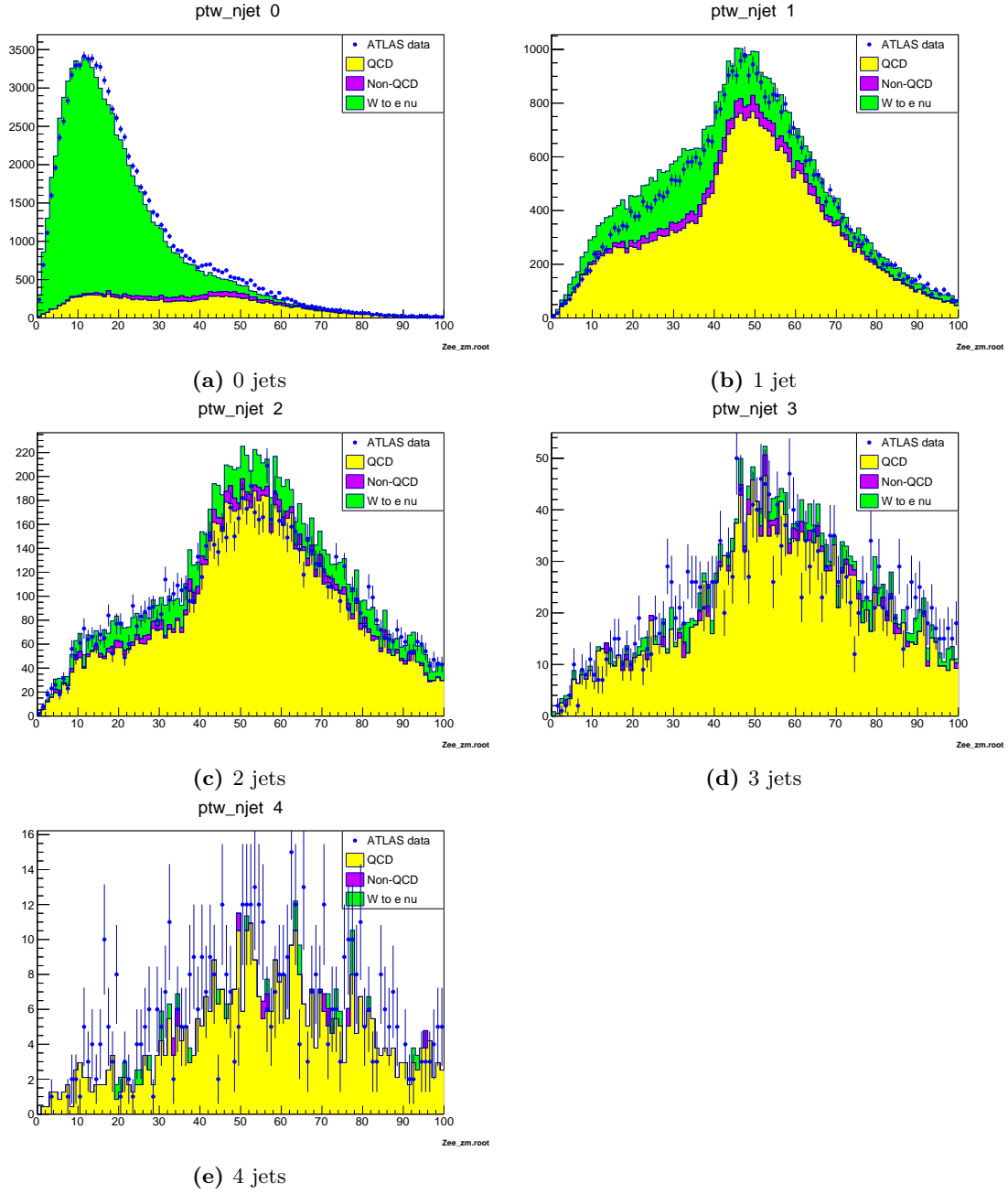


**Figure 3:**  $ptw$  distributions for different number of jets measured in the events

### 1.2.2. Final QCD scale factor

After examining the different kinematic variables, a final QCD scale factor has to be chosen. In order to do so, a region with high QCD background is chosen. For this we used the distribution of  $\mathbf{ptw}$ , since the signal consists mostly of QCD background for energies larger than around 30 GeV, as can be seen in figure 2. Therefore the cut

$$\mathbf{ptw} > 30 \text{ GeV}$$

is applied. To further increase the background, only events where the number of jets is larger than zero are taken into account, since we can see from figure 3, that the background to signal ratio increases for events with more than one jet. Therefore the cut

$$\mathbf{njet} > 0$$

was also applied. When looking at the two remaining kinematic variables,  $\mathbf{el\_pt}$  and  $\mathbf{etmis}$  in figure 2, it can be observed, that for momenta lower than 30 GeV, the background dominates the signal. Therefore the cuts

$$\mathbf{el\_pt} < 30 \text{ GeV}$$

$$\mathbf{etmis} < 30 \text{ GeV}$$

were also applied. The resulting distribution for different QCD scale factors can be seen in figure 4. The optimal value where the agreement between real and simulated data was identified by eye at  $c_{QCD} = 0.35$ . The  $\mathbf{ptw}$  distribution for that scale factor can be seen in part (b) of figure 4. To determine the error bounds of the QCD scale factor, the QCD scale factor was varied until the simulated and real data deviated visibly. The final QCD scale factor was then chosen as

$$c_{QCD} = 0.35^{+0.04}_{-0.05}$$

Since this entire process was only done per eye, this result is highly subjective. However, in the following step, the background will be reduced as much as possible, therefore the QCD scale factor does not have a very large impact on the final result of  $m_W$ .



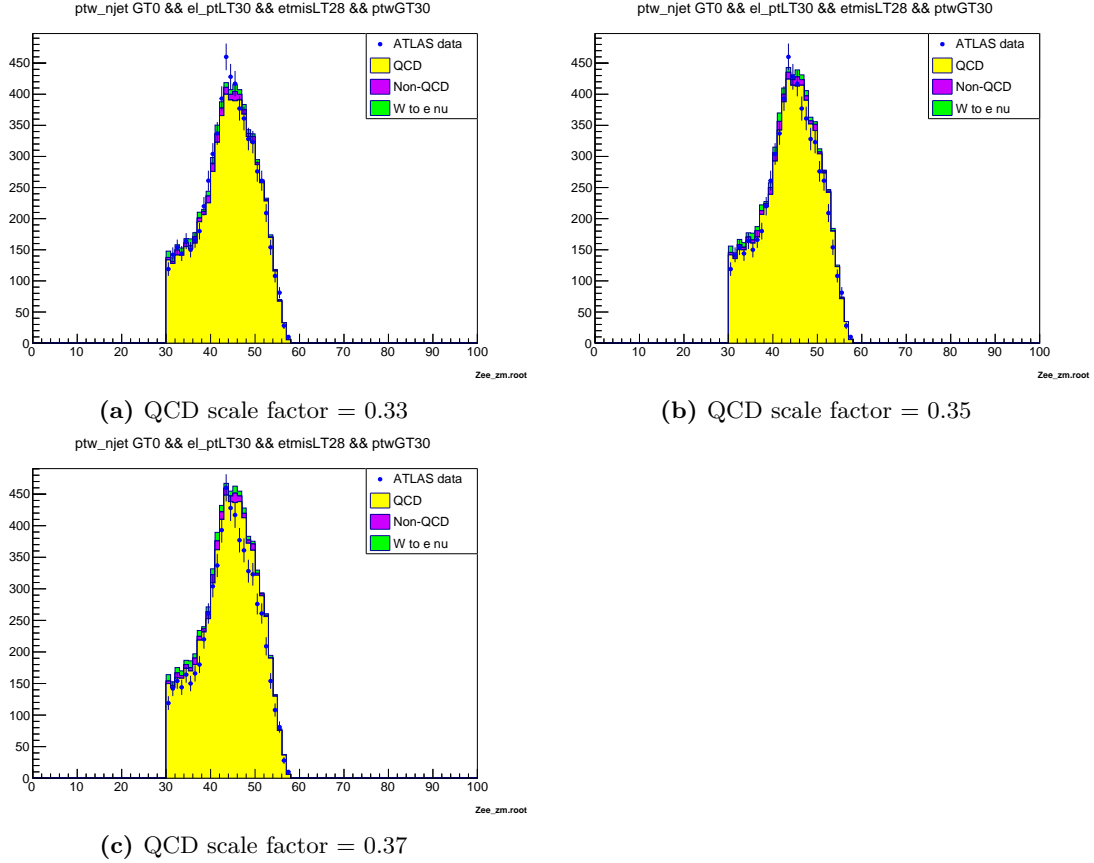


**Figure 4:**  $ptw$  distributions with the cuts  $ptw > 30$  GeV,  $njet > 0$ ,  $el\_pt < 30$  GeV and  $etmis < 30$  GeV for different QCD scale factors

### 1.3. Cut selection

In order to achieve the most accurate  $m_W$  a cut selection has to be applied, so that the distribution of the  $el\_pt$ , which is used to calculate  $m_W$ , has the highest signal to background ratio. In order to choose the proper cut selections, the distributions of the kinematic variables in figures 2 and 3 are examined again. The following cuts were chosen:

Since there are no jets expected in  $W \rightarrow e\nu$  events, which can be confirmed when looking at figure 3 where the signal to background ratio decreases significantly as the number of jets increases, the cut  $njet == 0$  is applied.

Since there is a neutrino present in the  $W$  decay, missing transverse momentum/energy  $\cancel{E}_T$  is expected in the events. When looking at the  $etmis$  distribution in figure 6, the background is largest for small  $\cancel{E}_T$ . After some trial and error, the cut  $etmis > 33$  GeV is chosen.

It is expected, that the  $W$  boson itself does not have a large transverse momentum, which can be confirmed when looking at the  $\text{pt}_W$  distribution in figure 6. Therefore events with large  $\text{pt}_W$  are cut off. The final cut was chosen as  $\text{pt}_W < 35 \text{ GeV}$ .

So the final cut

$$\text{njet} == 0 \ \&\& \ \text{et}_{\text{mis}} > 33 \ \&\& \ \text{pt}_W < 35$$

is applied to the  $\text{e1}_{\text{pt}}$  distribution. The distribution of  $\text{e1}_{\text{pt}}$  with the cuts applied can be seen in figure 5

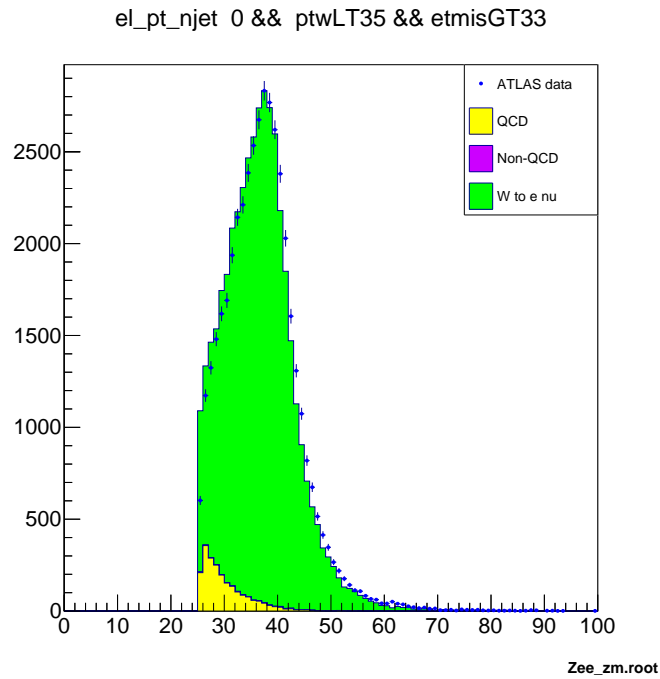


**Figure 5:** Electron transverse momentum  $\text{e1}_{\text{pt}}$  with the cuts  $\text{njet} == 0 \ \&\& \ \text{et}_{\text{mis}} > 33 \ \&\& \ \text{pt}_W < 35$  applied.

When comparing the  $\text{e1}_{\text{pt}}$  distribution with the cuts and the final QCD scale factor applied, to the  $\text{e1}_{\text{pt}}$  distribution in figure 6, the agreement between simulated and real data is increased whilst the background is decreased significantly. Therefore the applied cuts as well as the QCD scale factor seem to be a decent choice.

#### 1.4. Gauge curves

#### 1.5. W-mass

### A. Appendix

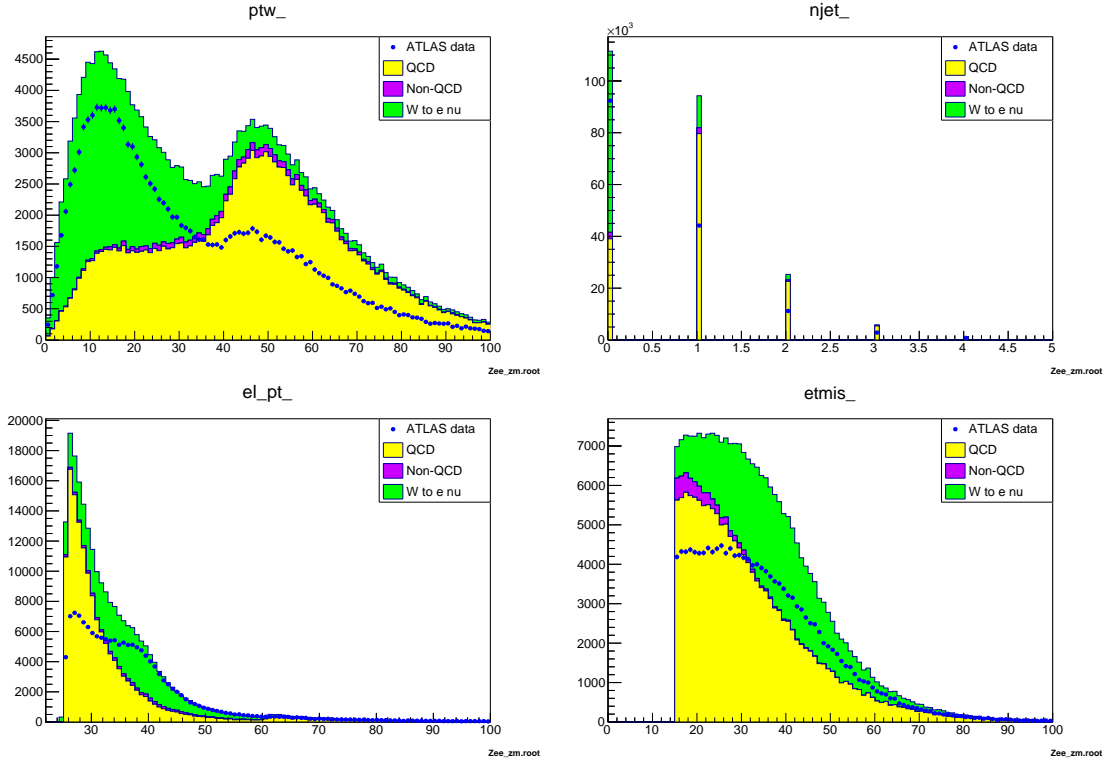


**Figure 6:** Distributions of the kinematic variables  $ptw$ ,  $njet$ ,  $el_{pt}$  and  $etmis$  for a QCD scale factor of 1

## References

- [1] Physikalisches Institut University Bonn. *Instruction manual*. 2025.